



Modeling of temperature field and grain growth of a dual phase steel DP980 in direct diode laser heat treatment

Fanrong Kong, S. Santhanakrishnan, Dechao Lin, Radovan Kovacevic*

Research Center for Advanced Manufacturing, Southern Methodist University, 3101 Dyer Street, Dallas, TX 75205, USA

ARTICLE INFO

Article history:

Received 23 April 2009

Received in revised form 16 July 2009

Accepted 17 July 2009

Keywords:

Heat treatment

Heat-affected zone (HAZ)

Dual phase steel

Finite element method (FEM)

Monte Carlo (MC) method

ABSTRACT

The temperature field due to heating from a high-powered direct diode laser is calculated first by using an experiment-based finite element model. The Monte Carlo method is applied, which uses the calculated temperature history as thermal loading to obtain the grain growth in the heat-affected zone (HAZ) of dual phase steel DP980. The martensite decomposition in the heat treatment is considered to be a function of the scanning speed. Numerical results demonstrate that the increased scanning speed of the laser beam under laser power of 2 kW decreases the temperature gradient in the HAZ, resulting in finer martensite grains and a smaller percentage of martensite decomposition in the HAZ. This is in good agreement with the experimental data.

© 2009 Elsevier B.V. All rights reserved.

1. Introduction

In recent years, dual phase (DP) steel, characterized by the ferrite phase as the matrix and martensite as the dispersion, is finding application in the automobile industry because it has advanced high strength, good formability, high energy absorption, and reduced density. However, this material has a problem if a welding process is used. Naturally, the formability and toughness of welded joints are much lower than those of the corresponding parent material. The loss of formability and toughness is linked to the presence of a soft zone in the outer region of heat-affected zone (HAZ) in the joint, which has been reported by Xia et al. (2007). Lin et al. (2008) applied a hybrid laser-tungsten inert gas (TIG) welding technique to join a gap-free galvanized steel DP980, and also find that a lower hardness exists at the HAZ with respect to the base metal. Heat treatment by using a direct diode laser can restore joint toughness but causes a loss of the joint strength because the martensite both in the weld and HAZ is tempered, as described by Capello et al. (2007). Because the mechanical properties of welded joints strongly depend on the microstructure of the weld and HAZ, the grain growth in these two areas should be investigated. Conventional techniques in the evaluation of the martensite phase in the steel, such as using a scanning electron microscope (SEM) and transmission electron microscope (TEM), are difficult to apply to the structural evolution that occurs during weld

solidification at elevated temperatures. Recently, the development of advanced computational science gives us a means to simulate those grains' growth by developing a thermal-microstructure model. Great achievements have been made in the simulation of the grains' growth or crystals' evolution in the casting, laser welding, and arc welding process by applying the Monte Carlo model in cooperation with thermal analysis that uses the finite difference method or finite element method. The advantage of this thermal-microstructure model is that the temperature field analysis and the coupled microstructure simulation can be performed simultaneously. Gao and Thompson (1996) earlier presented a real time-temperature model for MC modeling of normal grain growth in metal and alloys, in which an experimental data-based (EDB) model is used to couple the MC simulation with experimental grain growth data. Li and Kannatey-Asibu (2002) applied Monte Carlo technique to simulate the grain structure evolutions in HAZ during welding of a nickel 270 steel, and find that a linear relationship exists between the average grain size and the average number of sides of grains. Sista et al. (2002) used a three-dimensional (3D) Monte Carlo model to predict the evolution of the grain structure and topological class distributions in zone-refined iron. Kazutoshi et al. (2003) carried out Monte Carlo simulation of grain growth and recrystallization behaviors in HAZ for gas tungsten arc (GTA) and laser beam (LB) weldments of carbon steel and nickel. The temperature distribution in HAZ is analytically computed by quasi-stationary heat conduction equations. Mishra and Debroy (2004) calculated the grain size and topological class distributions in the HAZ of a gas tungsten arc welded Ti-6Al-4V alloy by using a 3D Monte Carlo model. The thermal history is obtained from an

* Corresponding author. Tel.: +1 214 768 4865; fax: +1 214 768 0812.
E-mail address: kovacevi@lyle.smu.edu (R. Kovacevic).

experimentally verified numerical heat transfer and fluid flow model. Shi et al. (2004) studied the evolution of grain structure in weld HAZ of the ultra fine grain steel under welding thermal cycle by using an integrated 3D Monte Carlo simulation system. Raabe et al. (2004) further reviewed the application of Monte Carlo model in the continuum scale modeling of material processing techniques. Wei et al. (2007) presented a heat transfer and fluid flow model combined with MC simulation to study the stainless steel SUS316 grain growth in HAZ of gas tungsten arc welding (GTAW) process. Wang et al. (2005) used a finite element method to calculate the temperature field in the flash welding process with a thermal–electrical coupled model, followed by an investigation into the austenite grain growth in HAZ. Kazeminezhad et al. (2007) presented a finite element model combined with the Monte Carlo method to simulate the distribution of grain size in the annealing of an inhomogeneously deformed copper wire, in which a finite element method is used to calculate the stored energy distribution due to the deformation. The temperature results are then applied as input in the Monte Carlo model to determine the distribution of grain size. All the models mentioned above used a same assumption that the grain in the material is a single crystal. There are no published results on the simulation of the microstructure of multiple-phase materials up to now. This paper focuses on the development of a thermal-microstructure model to simulate the microstructure of HAZ of dual phase steel DP980. A high-power direct diode laser is used as a heating source, and the martensite decomposition in the HAZ is considered.

2. Establishment of the mathematical modeling

2.1. Thermal analysis of the heat treatment by direct diode laser

During the heat treatment, the material properties have a strong relationship with the maximum generated temperature. Therefore, to numerically predict the microstructure or the evolution of grain growth in the process, the calculation of the on-going temperature field is necessary. In this study, the transient temperature distribution is calculated by the finite element method, and the maximum temperature in the laser heated zone is lower than the melting point of steel. The boundary conditions include: (1) the heat input from laser radiation at the top surface and (2) the heat loss due to convection and radiation on all surfaces of the specimen.

Because the convection inside of the coupon does not exist in the heat treatment process, the energy conservation equation can be simplified by ignoring the convection term as follows:

$$\frac{\partial(\rho c T)}{\partial t} = \frac{\partial^2(kT)}{\partial x^2} + \frac{\partial^2(kT)}{\partial y^2} + \frac{\partial^2(kT)}{\partial z^2} \quad (1)$$

Here, ρ is the density of material considered, c is the specific heat, and k is the thermal conductivity.

The boundary conditions at the top surface include the heat losses due to the convection and radiation and heat input from the moving heat source as given by:

$$k \frac{\partial T}{\partial y} = q_{\text{laser}}(x, y, z) - \sigma \varepsilon (T^4 - T_{\infty}^4) - h_c (T - T_{\infty}) \quad (2)$$

Here, $q_{\text{laser}}(x, y, z)$ is the heat input from laser radiation, σ is the Stefan–Boltzman constant ($\sigma = 5.67 \times 10^{-8} \text{ W/m}^2/\text{K}^4$), ε is emissivity, T_{∞} is the room temperature, and h_c is the forced convection coefficient due to the shielding gas.

Because the diode laser is characterized with a rectangular beam (see Fig. 1) and a uniform energy distribution (Capello et al., 2007),

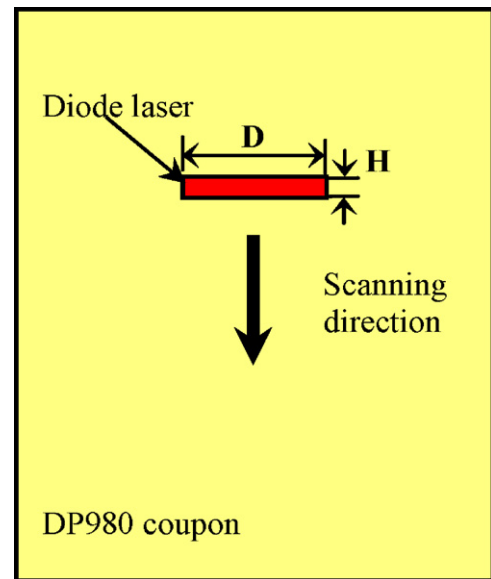


Fig. 1. Schematic view of laser heat treatment.

the laser energy can be described as:

$$q_{\text{laser}}(x, y, z) = \begin{cases} \frac{\eta P_l}{DH} & y = L_w, |x - x_0| \leq D/2, vt < z < vt + H, \\ 0 & \text{other} \end{cases} \quad (3)$$

where, x , y , and z are the 3D coordinates, η is the absorption efficiency of laser by the material, x_0 is location of laser beam center along the x coordinate, P_l is the laser power, L_w is the overall thickness of the coupon, D is the effective length of the focused laser beam, H is the focused laser width, t is the time, and v is the laser scanning speed.

The boundary conditions at the other surfaces are given by:

$$-k \frac{\partial(T)}{\partial n} = \sigma \varepsilon (T^4 - T_{\infty}^4) + h_c (T - T_{\infty}) \quad (4)$$

Here, n is the normal outward vector to the surface of specimen.

2.2. Simulation of grain growth in heat-affected zone of a dual phase steel DP980

The Monte Carlo methodology to simulate the grain growth is described in detail in the literatures (Wang et al., 2005; Gao and Thompson, 1996; Raabe et al., 2004; Shi et al., 2004; Li and Kannatey-Asibu, 2002). The concept of the Monte Carlo method to simulate grain growth is relatively simple but fascinating. The only basic requirement of this method is knowledge of the thermodynamics of atomic interactions. The first step is to represent the considered material as a 2D or 3D matrix in the form of surface or volume elements. The content of each element represents its crystallographic orientation. The sets of equal elements represent bigger grains as schematically shown as the 2D structure in Fig. 2.

The grain boundaries among single grains are fictitious surfaces that separate volumes with different orientations. After choosing the matrix type and filling it initially with random numbers, the simulation process can start. These are four primary steps in the mathematical algorithm:

- (1) Calculate the free energy of an element in the matrix (G_i) with its specific crystallographic orientation (S_i) based on its surroundings.
- (2) Randomly select a new crystallographic orientation for element (S_f).

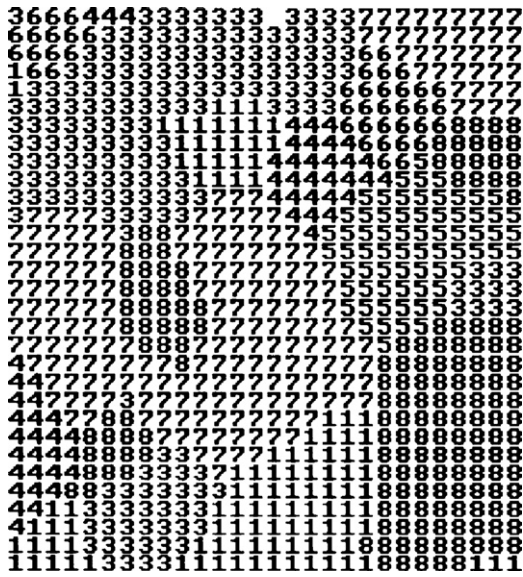


Fig. 2. The grain structure in MC model.

- (3) Calculate again the free energy of the new-coming element (G_f) with the new crystallographic orientation (S_f).
- (4) Compare the two energy values and find their difference of $G_f - G_i$. A new-grain orientation that minimizes the free energy is created with the selected transition probability W .

These four steps are repeated millions of times at random positions in the matrix. The eventual result is a microscopic simulation of the free energy decay in the system, which is actually the main driving force for grain growth. The Hamiltonian that describes the interaction among the closest neighbors in an element represents the grain boundary energy expressed as:

$$G = -J \sum_{nn} (\delta S_i S_j - 1) \quad (5)$$

where, J is a positive constant that sets the scale of the grain boundary energy, S_i is one of the possible orientations in the i th element in the matrix, S_j is one of neighboring elements' crystallographic orientation, nn denotes the amount of neighboring element for each element. In this MC model, a Moore neighborhood model is chosen; therefore, the value for nn is set at 8. δ_{ab} is the Kronecker-delta, which becomes 1 when two elements in the matrix are equal and 0 for others. As a result, neighboring elements with a different orientation contribute a free energy J to the system and 0 with the same orientation.

The transition probability W is given by:

$$W = \begin{cases} \exp\left(-\frac{\Delta G}{k_b T}\right), & \Delta G > 0 \\ 1, & \Delta G \leq 0 \end{cases} \quad (6)$$

where, ΔG is the change in free energy due to the orientation alteration, k_b is the Boltzman constant, and T is the temperature. Therefore, the speed of the moving segment can be obtained:

$$v_i = C_1 \left[1 - \exp\left(-\frac{\Delta G}{k_b T}\right) \right] \quad (7)$$

where, C_1 is the boundary mobility.

For a continuous grain growth, the final grain size can be calculated by using the following equation (Sista et al., 2002):

$$L^n - L_0^n = f(T)t \quad (8)$$

where L_0 and L are the initial and final mean grain sizes calculated with the linear intercept method, respectively, n is the grain growth exponent, and $f(T)$ is generally given as an Arrhenius-type equation (Sista et al., 2002). Its expression can be shown as follows:

$$f(T) = K \exp\left(-\frac{Q}{RT}\right) \quad (9)$$

where, K is the pre-exponential coefficient, R is the gas constant, and Q is the activation energy for grain growth.

The Monte Carlo method is proven to be an effective way to simulate grain growth at a constant temperature gradient or in a situation with slow and uniform temperature evolution such as the application in the casting of large parts (Wei et al., 2007). In the heat treatment by laser, there exists a dynamic thermal process with rapid heating and cooling resulting in an abrupt temperature gradient in the heat-affected zone. In the simulation of microstructure evolution, three techniques named with the atomistic models, a grain boundary migration (GBM), and experimentally data-based (EDB) models, are developed (Wang et al., 2005; Gao and Thompson, 1996; Raabe et al., 2004; Li and Kannatey-Asibu, 2002). The atomistic model can only be applied to small assemblies of atoms such as nanocrystals (Gao and Thompson, 1996); it is not suitable for a large-scale HAZ simulation. The GBM model is good for grain-growth simulation when the isothermal grain-growth kinetics is not available. However, the physical properties of the material in this model have to be available, and the grain size is assumed to be proportional to the square root of time. In addition, the assumed grain growth exponent of 0.5 is not appropriate for many engineering alloys (Gao and Thompson, 1996).

The EDB model can avoid this shortage and be applied to simulate the HAZ grain growth when the isothermal grain-growth kinetics of a material is available. Therefore, it can be used to relate time and temperature to the Monte Carlo simulation-time step t_{MCS} :

$$L = K_1 \lambda (t_{MCS})^{n_1} \quad (10)$$

where λ is the discrete grid-point spacing in the Monte Carlo technique, and K_1 and n_1 are constants. Through the regression calculation of t_{MCS} and the Monte Carlo method simulating the grain size, the values of K_1 and n_1 are derived as 0.715 and 0.477, respectively (Mishra and Debroy, 2004). In the EDB model, the relationship between the t_{MCS} and the real time-temperature $T(t)$ is expressed as follows (Gao and Thompson, 1996):

$$(t_{MCS})^{m_1} = \left(\frac{L_0}{K_1 \lambda}\right)^n + \frac{K}{(K_1 \lambda)^n} \sum \left(\exp\left(-\frac{Q}{RT(t)}\right) \Delta t_i\right) \quad (11)$$

where $T(t)$ is the mean temperature in a time interval Δt_i . Therefore, at any given monitoring location where the temperature is known as a function of time, t_{MCS} can be related to the real time t , which is $\sum \Delta t_i$. The t_{MCS} values at different locations, calculated from Eq. (11), cannot be directly applied to the Monte Carlo algorithm because the choice of a grid point for updating the orientation number is random in the Monte Carlo (MC) technique. Thus, the probability of selecting each grid point is the same as in the traditional MC calculations. However, grains must grow at higher rates in the HAZ regions of higher temperature, where a steep temperature gradient exists. This fact must be included in any realistic grain-growth calculation scheme. One way is to devise a scheme where grain orientations at higher-temperature locations (higher t_{MCS} locations) are updated with a higher frequency by considering a probability gradient. That is, the site-selection probability varies with location. The larger the t_{MCS} at a site, the higher the corresponding site-selection probability (Wei et al., 2007; Gao and

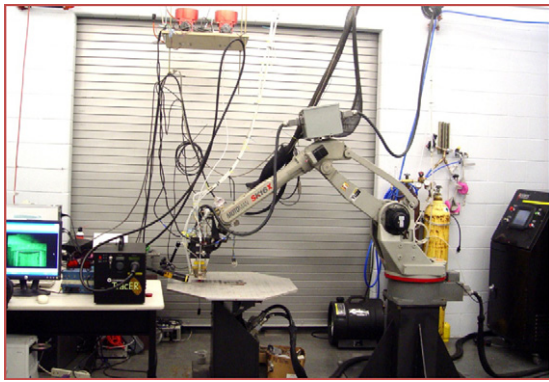


Fig. 3. Experimental setup of laser heat treatment.

Thompson, 1996):

$$P = \frac{t_{MCS}}{t_{MCSMAX}} \quad (12)$$

Here, t_{MCSMAX} is the maximum of t_{MCS} in the simulation domain.

Previous experimental work on the heat treatment of dual phase steel DP980 by using a diode laser shows that the microstructure in the fusion zone and adjacent HAZ consists of ferrite and martensite phases. The ferrite serves as the matrix, and the martensite as dispersion through that matrix. The hardness testing shows that the softened region is in an outward area of HAZ toward the base material. The softening can be contributed to the tempering of the martensite phase. SEM observation in the HAZ shows that martensite in this area is decomposed to visible carbides (Xia et al., 2007). Based on this report, an assumption that the martensite phase can decompose only in the heating process is considered in this model. This similar assumption is proposed by Costa et al. (2005) in grain-growth kinetics, where the percentage of decomposed martensite depends on the dwelling time in the martensite decomposition temperature range. A detailed procedure of modeling the martensite decomposition can be described in the following two steps:

- (1) Define the initial type number of grains in each grid. The initial number is 1 when it belongs to the martensite with the probability of P_1 ; otherwise, it is 0. Here, P_1 is assumed as an initial weight ratio of the martensite in dual phase steel.
- (2) Randomly select a new crystallographic orientation for each element, and calculate again the free energy of the new-coming element. A new-grain orientation that minimizes the free energy is created with the selected transition probability W . When the new-grain orientation is accepted and belongs to the martensite crystal with $\Delta T/\Delta t > 0$, new-grain growth stops. Otherwise, the new-grain growth is accepted and a next calculation begins.

By integrating these two steps into the Monte Carlo algorithm mentioned above, and setting up the initial martensite and ferrite weight ratio to be 60 and 40%, respectively (Sederstrom, 2007), the distribution of martensite and its evolution can be obtained.

2.3. Experimental and numerical procedures

A diode laser with a full power of 2 kW is used in the experimental set-up, as shown in Fig. 3. DP980 steel is used for the coupons with a geometrical size of 50 mm × 50 mm × 2 mm. The laser scanning speed is set as 8–20 mm/s, the efficient usage of laser power is 76%, and the heating size of the laser beam is 12 mm × 0.5 mm. All the welding experiments are performed at the robotized welding cell. Thermocouples are fixed at the surface near the heated zone

to measure the temperature evolution. The acquired temperature data is then used for the validation of the simulation results.

The numerical procedure is implemented based on finite element (FE) code ANSYS11.0. The main thermal properties of DP980 steel are shown in Table 1 (Xia et al., 2008). All the procedures are implemented based on ANSYS Parametric Design Language (APDL). The thermal conduction element, named SOLID70 in ANSYS, is chosen because of its excellent ability for the 3D transient thermal analysis (ANSYS Inc., 2007). The geometrical size of the coupons for simulation and experiment is the same. In this study, un-uniform meshes are used, as shown in Fig. 4. The finer mesh is placed near and along the weld bead to assure the accuracy of the simulation, and the courser mesh is used for the rest of the metal sheet in order to reduce the computation cost. A 100 × 100 grid is chosen in the transverse section of the weld to model the grain growth in the HAZ. It is assumed that the grain growth in the HAZ is two-dimensional and the influence of the longitudinal orientation of grain growth along the scanning speed is ignored in this study. The Monte Carlo model is programmed by using Matlab software.

3. Results and discussion

3.1. Experiment-based thermal analysis of heat treatment by direct diode laser

A thermal analysis, shown in Fig. 5, demonstrates the temperature evolution in the heat treatment of dual phase steel DP980 with a direct diode laser of 2000 W in power and with a travel speed of 20 mm/s. Fig. 5a shows the temperature profile at the beginning of the heat treatment ($t = 0.6$ s), while Fig. 5b shows the temperature profile at $t = 1.3$ s, and Fig. 5c shows the temperature profile at the end of the treatment process at $t = 2.4$ s. Because the laser beam has a 12 mm × 0.5 mm rectangular profile, the top surface of the substrate is quickly heated to a high temperature and generates a narrow laser-material interaction zone, which is marked by an arrow in Fig. 5a. From these three figures, it is seen that the width of the heat-treated zone stays unchanged, where the maximum temperature is slightly higher at the end (from 1363 °C at $t = 0.6$ s to 1417 °C when $t = 2.4$ s). Therefore, the steady state of the temperature, located in the middle area of heat-treated zone is selected as the heat input in the following Monte Carlo simulation.

To verify the temperature simulation, a machine-vision system consisting of a CCD camera, an appropriate filter assembly, and a green laser of 532 nm in wavelength for the illumination source, is used to capture the image of the interaction zone of the laser and material in real time with a typical picture shown in Fig. 6a. In this

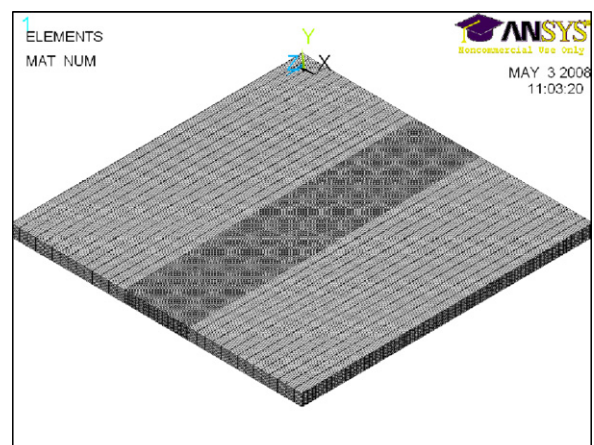


Fig. 4. Finite element mesh.

Table 1
Main physical property of DP980 steel.

Material property	Density (kg/m ³)	Specific heat capacity (J/kg K)	Thermal conductivity (W/m K)
Value	7860	680	30

figure, the interaction zone is located between the treated zone and the un-treated zone. A pair of thermocouples is attached close to the treated zone for the temperature verification, which are set at the top surface 10 mm distance from the centerline of heat-treated zone. The numerically obtained temperature results for the selected process parameters are displayed in Fig. 6b. The temperature distribution of a numerical simulation and the thermocouple reading at the same point are summarized in Fig. 6c. It can be observed from

this figure that the numerical analysis and experimental observations are in good agreement. In this case, the numerical calculation shows that the maximum temperature under the laser-material interaction zone is 1373 °C, which is lower than the melting point of DP980 (around 1500 °C) (Lin et al., 2008). A post-process visual inspection confirms that the surface is not melted. The temperature contour at the cross-section is shown in Fig. 7a. It can be seen that the heat-affected zone generated by the direct diode laser is of a

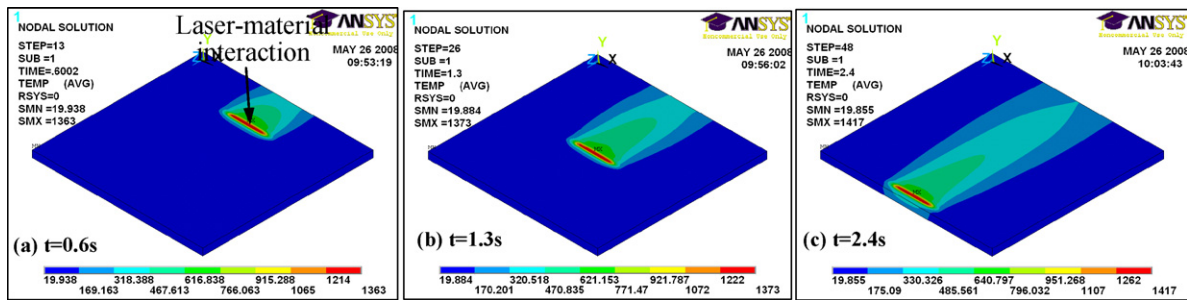


Fig. 5. Temperature evolution in the heat treatment with laser scanning speed at 20 mm/s.

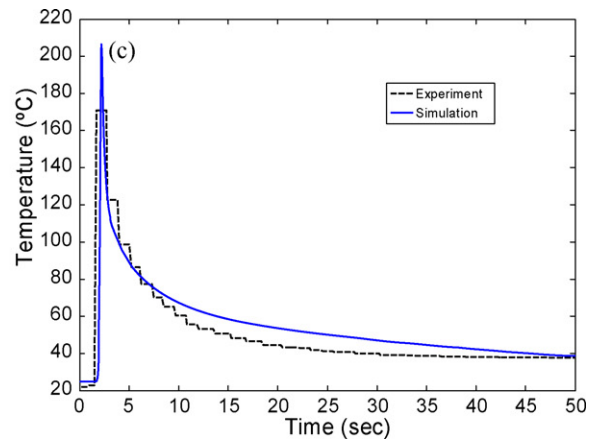
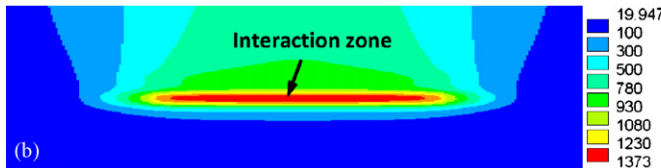
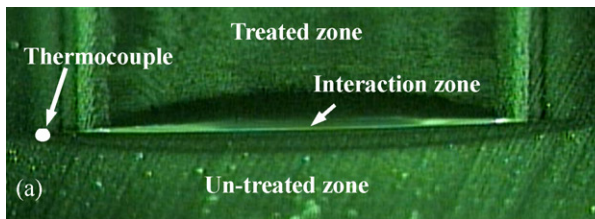


Fig. 6. Heat treatment at laser power of 2000 W and speed at 20 mm/s. (a) Real-time observation of the laser-material interaction zone, (b) numerical thermal analysis, (c) temperature distribution at the point thermocouple located in 6a.

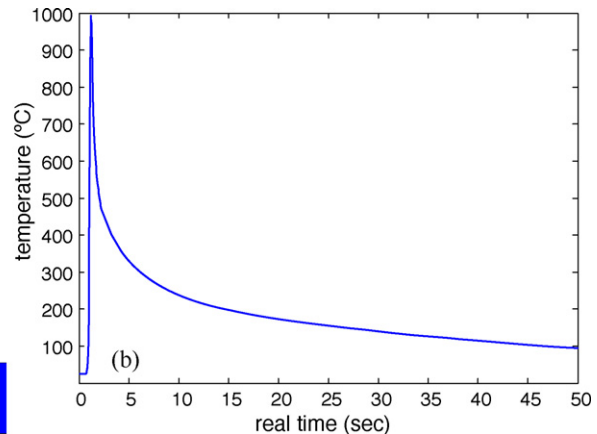
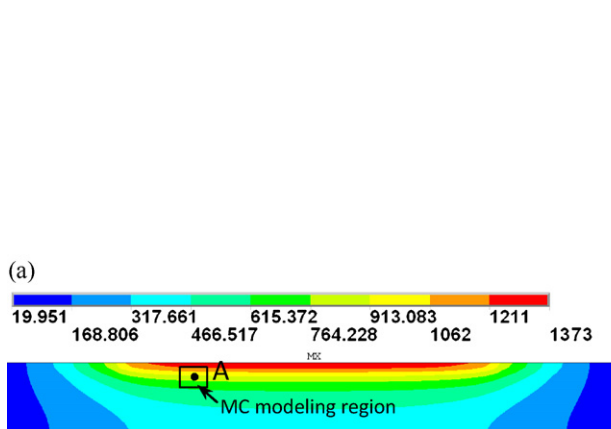


Fig. 7. The cross-section of a heated zone (a) temperature contour and (b) temperature history at point A marked in 7a.

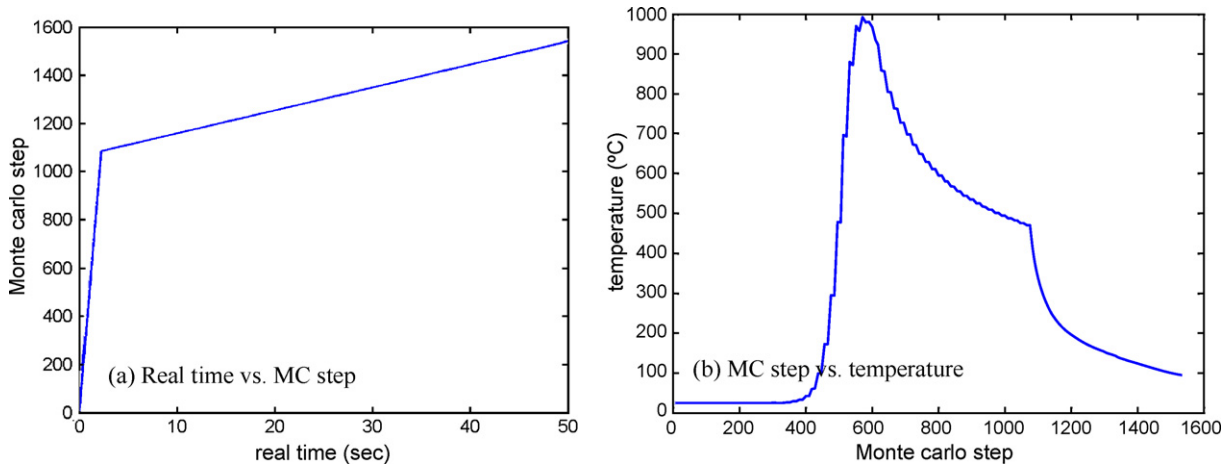


Fig. 8. The relationship of the MC step with real time and temperature at position A.

wide width and shallow depth. The temperature history shown in Fig. 7b is used in the Monte Carlo model as the thermal load. Due to characteristic of direct diode laser radiation, the heating phase of the coupon occurs at a short time interval by reaching a high temperature quickly. The heating phase is followed by a long and uniform cooling period. The cooling rate mainly decides the final microstructure morphology.

3.2. Modeling the grain growth in the heat treatment process

The temperature history from the thermal analysis, which is also validated by the experimental measurement, is used as the thermal load for the Monte Carlo model to study the crystal evolution of the HAZ according to Eq. (11). The relationship of the Monte Carlo step with respect to real time and temperature is shown in Fig. 8.

The relevant location for the MC model at the HAZ in this study is shown in Fig. 7a for the numerical model (position “A”) and Fig. 9b for experimental verification (MC modeling region). In this study, the initial grain size is set to 10 μm, the grid configuration is 100 × 100, and the grid spacing is also 10 μm. Therefore, the unit length of the Monte Carlo modeling area is equal to 10 μm × 100 = 1.0 mm. The other related Monte Carlo model parameters used in this study are given in the Reference (Mishra and Debroy, 2004). The numerical results show that the heat-treated depth in thermal analysis (Fig. 9a) matches well with the experimental result (Fig. 9b).

Based on the validated thermal analysis, the Monte Carlo model is used to systematically simulate the grain growth and martensite decomposition in the laser heating and cooling process. Fig. 10a shows the microstructure of HAZ in heat-treated DP980 steel using

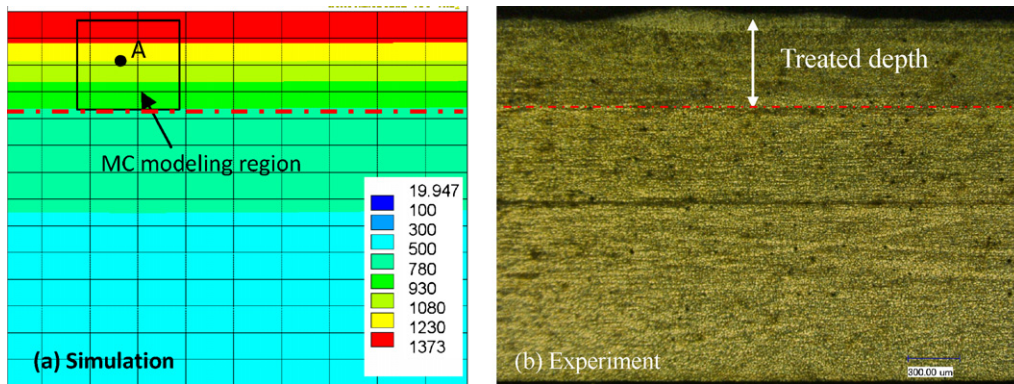


Fig. 9. Numerical simulation (a) and experimental measurement (b) of heat-treated depth of DP 980 steel.

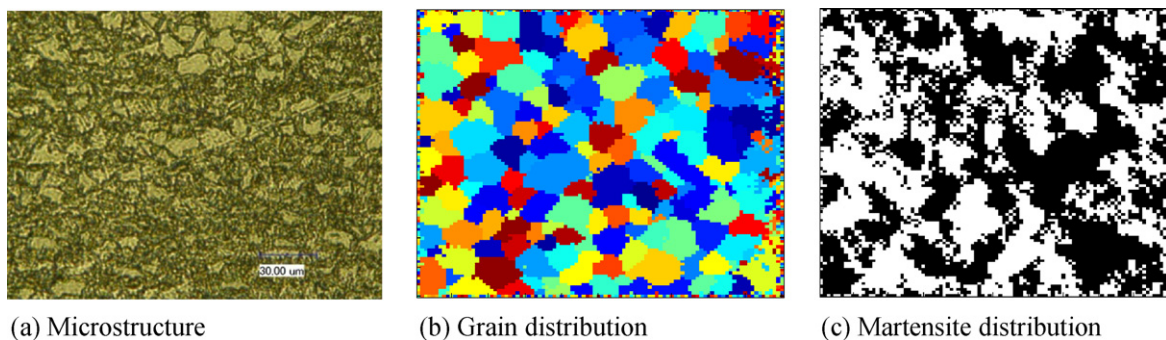


Fig. 10. Experimental and numerical results of the microstructure growth in the HAZ. (a) Microstructure, (b) grain distribution, (c) martensite distribution.

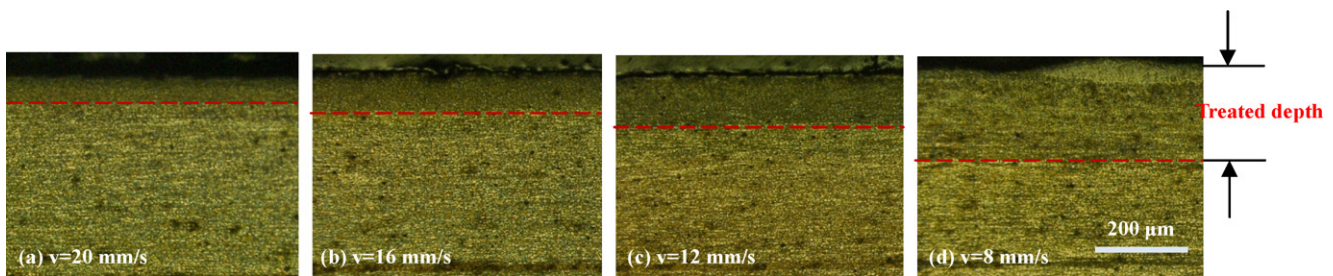


Fig. 11. The cross-sectional views of heat-treated zone of DP980 steel obtained by optical microscope at variable laser scanning speeds.

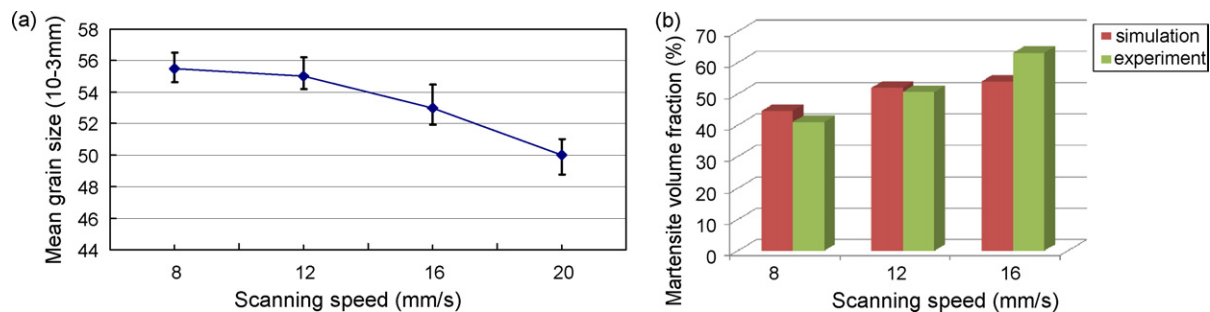


Fig. 12. Influence of laser scanning speed on the mean grain size (a) and martensite volume fraction (b) in HAZ of DP980 steel.

optical microscopy at 1000 times magnification. Fig. 10b shows the Monte Carlo modeling results of the grain distribution (including the ferrite and martensite) at the corresponding location. The error of the grain size between experimental and numerical results is about 15%. The final martensite distribution in the HAZ is also shown in Fig. 10c, in which the white zone denotes martensite.

In this study, four scanning speeds with a constant power of laser at 2 kW are considered by studying the influence of the laser scanning speed on the microstructure in the heat-treated zone of DP980 steel. The increase of the scanning speed reduces the temperature at the fixed location of the coupons. At the same time, the depth of the heat-treated zone decreases accordingly; the relevant experimental photos of cross-sectional views of heat-treated zone are shown in Fig. 11. The numerical analysis indicates that with the increase of the scanning speed, the mean value of grain size decreases accordingly, as shown in Fig. 12a. It can be seen that by increasing the scanning speed with the fixed laser power, the heat-treated depth in the specimen is reduced (see Fig. 11) and the martensite volume fraction in the heat-treated zone is also increased accordingly, as shown in Fig. 12b.

4. Conclusions

A thermal-microstructure model, as a combination of the finite element method with the Monte Carlo model (FE-MC), is developed to study the heat transfer and grain evolution processes in the heat-treated zone of dual phase steel DP980 by direct diode laser. The following can be concluded from this work:

- (1) The thermal distribution and temperature history directly influence the grain-growth evolution. The simulation has a qualitative agreement with the experimental observation.
- (2) The martensite decomposition in the HAZ is considered under various temperature gradients. With the increase in scanning speed, the temperature gradient in the HAZ and the heat-treated depth decreases; thereby, the mean grain size of martensite becomes finer and the percentage of martensite decomposition in the HAZ is smaller.

- (3) The developed model can be used to simulate the heat-affected zone in the laser welding of dual phase steel DP980.

Acknowledgement

Authors want to thank the National Science Foundation (NSF) for financial support under Grant No. EEC-0541952.

References

- ANSYS Inc., 2007. ANSYS 11.0 Manual.
- Capello, E., Castelnovo, M., Previtali, B., Vedani, M., 2007. Surface treatment of welded duplex stainless steels by diode laser. *Journal of Laser Applications* 19 (3), 133–140.
- Costa, L., Vilar, R., Reti, T., Deus, A.M., 2005. Rapid tooling by laser powder deposition: process simulation using finite element analysis. *Acta Materialia* 53, 3987–3999.
- Gao, J.H., Thompson, R.G., 1996. Real time-temperature models for Monte Carlo simulations of normal grain growth. *Acta Materialia* 44, 4565–4575.
- Kazeminezhad, M., Karimi Taheri, A., Kiet Tieu, A., 2007. Utilization of the finite element and Monte Carlo model for simulating the recrystallization of inhomogeneous deformation of copper. *Computational Materials Science* 38 (4), 765–773.
- Kazutoshi, N., Kazuyoshi, S., Naoyuki, T., Hiroaki, O., 2003. Monte Carlo Simulation for grain growth and recrystallization behaviors in HAZ of weldments. *Quarterly Journal of Japan Welding Society* 21 (2), 256–266.
- Li, M.-Y., Kannatey-Asibu, E., 2002. Monte Carlo simulation of heat-affected zone microstructure in laser-beam welded nickel sheet. *Welding Journal* 81 (3), 37–44.
- Lin, D., Yang, S., Huang, W., Kong, F., Kovacevic, R., Ruokolainen, R., Gayden, D.X., 2008. Development of hybrid laser/TIG welding process for gap-free galvanized steel DP980 at overlap joint configuration. In: 19th AeroMat Conference & Exposition, June 23–26, Austin, Texas, USA.
- Mishra, S., Debroy, T., 2004. Measurements and Monte Carlo simulation of grain growth in the heat-affected zone of Ti-6Al-4V welds. *Acta Materialia* 52, 1183–1192.
- Raabe, D., Roters, F., Barlat, F., Chen, L.-Q., 2004. *Continuum Scale Simulation of Engineering materials: Fundamentals-microstructures-Process applications*. Wiley Interscience, pp.77–98.
- Sederstrom, J.H., 2007. *Spot Friction Welding of Ultra High-strength Automotive Sheet Steel*. Master Dissertation. Brigham Young University.
- Shi, Y., Chen, D., Lei, Y., Li, X., 2004. HAZ microstructure simulation in welding of a ultra fine grain steel. *Computational Material Science* 31, 379–388.
- Sista, S., Yang, Z., Debroy, T., 2002. Three-dimensional Monte Carlo simulation of grain growth in the heat-affected zone of a 2.25Cr-1Mo steel weld. *Metallurgical and Materials Transactions* 31B, 529–536.

- Xia, M., Sreenivasan, N., Lawson, S., Zhou, Y., Tian, Z., 2007. A comparative study of formability of diode laser welds in DP980 and HSLA steels. *ASME Journal of Engineering Materials and Technology* 129, 446–452.
- Xia, M., Biro, E., Zhiling Tian, Y., Zhou, N., 2008. Effects of heat input and martensite on HAZ softening in laser welding of dual phase steels. *ISIJ International* 48 (6), 809–814.
- Wang, W., Shi, Y., Lei, Y., Tian, Z., 2005. FEM simulation on microstructure of DC flash butt welding for an ultra-fine grain steel. *Journal of Materials Processing Technology* 161, 497–503.
- Wei, Y., Xu, Y., Dong, Z., Xia, J., 2007. Three dimensional Monte Carlo simulation of grain growth in HAZ of stainless steel SUS316. *Key Engineering Materials* 353–358, 1923–1926.